WATER RESOURCES RESEARCH, VOL. 34, NO. 8, PAGES 1935–1940, AUGUST 1998

Evaluation of hydrodynamic scaling in porous media using finger dimensions

John S. Selker
Department of Bioresource Engineering, Oregon State University, Corvallis

Martin H. Schroth
Department of Civil, Construction and Environmental Engineering, Oregon State University, Corvallis

Abstract. The use of dimensionless scaling is ubiquitous to hydrodynamic analysis, providing a powerful method of extending limited experimetnal results and generalizing theories. *Miller and Miller* [1956] contributed a scaling framework for immiscible fluid flow through porous media that relied on consistency of the contact angle between systems to be compared. It is common to assume that the effective contact angle will be zero in clean sand material where water is the wetting liquid. The well-documented unstable wetting process of fingered flow is used here as a diagnostic tool for the scaling relationships for infiltration into sandy media. Through comparison of finger cross sections produced using three liquids as well as various concentrations of anionic surfactant, it is shown that the zero contact angle assumption is very poor even for laboratory cleaned silica sand: Experimental results demonstrate effective contact angles approaching 60°. Scaling was effective for a given liquid between sands of differing particle size. These results suggest that caution should be exercised when applying scaling theory to initial wetting of porous media by liquids of differing gas-liquid interfacial tensions.

1. Introduction

The power and appeal of the scaling laws introduced by *Miller and Miller* [1956] is the ability to quantitatively extend results of experiments made under one set of conditions to media of differing to grain size and to liquids of varying viscosities and/or interfacial tensions. This system of scaling is applied most commonly to compute unsaturated hydraulic conductivity and liquid retention between sets of similar media. In this application, only the is characteristic grain size of the various media is required. The same scaling analysis is well suited to understanding the time evolution of macroscopic processes, such as infiltration, evaporation, unstable wetting. Although many studies have validated scaling based on characteristic length [e.g., *Hillel and Elrick*, 1990], the predictive utility of scaling with viscosity, density, and interfacial tension has not been thoroughly investigated. The objective of this paper is to explore the quantitative predictions of Miller scaling of macroscopic dimensions with respect to characteristic particle grain size, liquid density, interfacial tension, and to a lesser degree viscosity. This was achieved using the Miller-scaling results for the dimensions of unstable wetting in air-dried sandy media as a diagnostic measure of macroscopic scaling predictions.

Fingered flow provides a very natural system for the investigation of macroscopic scaling relationships for flow through porous media. First, the process gives rise to well defined macroscopic features (fingers) which can easily be compared, with finger width being the primary feature of the unstable wetting process. Further, the linear stability analysis of J.-Y. Parlange and D. E. Hill has provided a robust predictive model for fingered flow [*Parlange and Hill*, 1976; *Glass et al.*, 1989; *Selker et al.*, 1992]. The equations presented by *Parlange and Hill* [1976] are readily scaled using the methods of *Miller and Miller* [1956] to obtain the scaling relationship for finger width given by

$$d_* = \frac{\rho g \lambda}{\sigma_{gl}} d \tag{1}$$

where ρ is the liquid density, g is the constant of gravitational acceleration, λ is the characteristic media length scale, σ_{gl} is the gas-liquid interfacial tension, d is the finger width in a given media, and d_* is the scaled finger width [*Glass and Nicholl*, 1996]. This expression is very convenient in that it is explicit in measurable parameters. In this paper we test this expression by varying λ through the use of four similar media, ρ through the use of three different liquids, and σ_{gl} by varying the imbibing liquid and adding an anionic surfactant to water.

A noteworthy feature of (1) is the lack of dependence on liquid viscosity. This reflects the fact that the forces affecting the finger dimensions are those generated by gravity (tends to make fingers smaller) and interfacial energies (as these increase, fingers become wider). For (1) to hold, the flux through the finger must be much less than the saturated conductivity of the medium (infiltration cannot be conductivity limited, under which circumstances the wetting front is stable).

2. Materials and Methods

Two types of experiments were performed. The primary data used to evaluate the scaling relationships were obtained from thin slab infiltration experiments. In these experiments a series of fingers of flow were generated in initially dry sands using a variety of fluid/sand combinations. A second set of supporting experiments was carried out investigating the effective contact

Paper number 98WR00625.
0043-1397/98/98WR-00625$09.00

Table 1. Selected Physical Properties of the Porous Media

Texture	Organic Carbon, g/kg	Porosity (s.d.)	d_{50} (s.d.), mm	K_{sat}, cm/min
12/20	0.3	0.34 (0.02)	1.105 (0.014)	30.19
20/30	0.4	0.34 (0.02)	0.713 (0.023)	15.02
30/40	0.3	0.35 (0.01)	0.532 (0.003)	8.94
40/50	0.3	0.36 (0.03)	0.359 (0.010)	4.33

All properties are as reported by *Schroth et al.* [1996] except porosity, which was measured in each packing. The parameter d_{50} is the grain size of the particle for which half of the mass of media has smaller particles; K_{sat} is the saturated hydraulic conductivity to water.

angle of liquid-solid interfaces by applying surfactant/water solutions to single grains of sand.

For the porous media, we selected the four Miller-similar silica sands described by *Schroth et al.* [1996], with grades identified as 12/20, 20/30, 30/40, and 40/50. These delineations refer to the standard mesh sizes which bound the particle dimensions from above and below. For complete hydrodynamic characterization and media preparation see work by *Schroth et al.* [1996]. The media consist of commercially sieved, washed, nearly spherical natural silica sand. The organic content of the sand is ≤0.04% for all media (Table 1).

To assess the wettability of the sands, individual grains were subjected to wetting from above by droplets generated by a fine gauge needle which was positioned using a microscope stand (Figure 1). The water droplet in this test had volume of 0.6 μL as dispensed using a micrometer plunger volumetric syringe. Individual grains of the 12/20 sand were attached to micropipettes with a solution of 10% FD&C blue dye 2 that had been spread as a thin film on a mailing envelope's water soluble adhesive strip. The pipettes tips were touched to the dye solution and then to the sand grains. The dried dye solution provided a strong bond between the sand and the capillary tube and allowed immediate visual detection of wetting of the grain of sand through a 12× hand lens as evidenced by the dissolution of the blue dye from the bond. Contact angle was deemed to be nonzero if there was no point of wetting reaching the blue dye bond within 30 s.

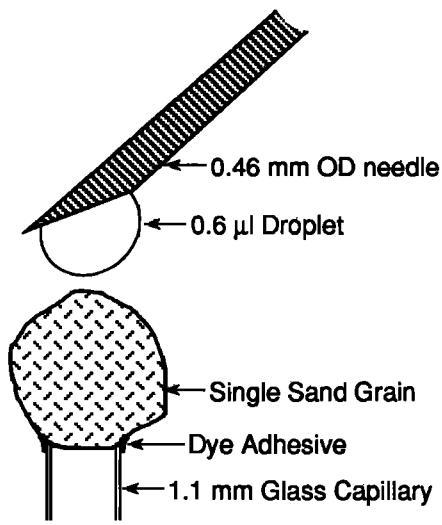

Figure 1. Experimental setup for individual grain measurement of wettability of sand.

Table 2. Selected Physical Properties of Liquids Employed

Liquid	Air/Liquid Interfacial Energy σ_{gl}, dyn/cm	Density ρ, g/cm^3	Viscosity, cP
Pore water	71.3	1.00	1.00
Duoprime 55	30.0	0.86	13.73
Soltrol 220	25.9	0.81	4.50

Properties are as measured at 23°C.

For our model liquids we employed distilled deionized water, which we refer to as pore water (after prolonged contact with the solid matrix), and two non–aqueous phase liquids (NAPLs), Soltrol® 220, which is a mixture of C_{13} to C_{17} branched alkanes (Phillips Petroleum Co., Bartlesville, Oklahoma), and Duoprime® 55 mineral oil (Lyondell Petrochemical Co., Houston, Texas). Gas-liquid interfacial tensions were measured by the ring method [*Du Noüy*, 1919], viscosities were measured using Ostwald viscometers [*American Society for Testing and Materials* (*ASTM*), 1995], and densities were provided by the manufacturer. All measurements were conducted at 23°C ± 0.5°C. The NAPLs provide interfacial tensions which differed from that of water by almost a factor of 3, densities which differed by about 20%, and viscosity's differing by more than a factor of 10 (Table 2).

The effects of variation in the gas-liquid interfacial tension were explored using a range of sodium dodecyl sulfate (SDS) surfactant solutions. All dilutions of SDS were maintained below the critical micelle concentration, beyond which little change is obtained in the gas-liquid interfacial tension [*Downey and Addison*, 1937]. The range of concentrations employed provided interfacial tensions between 37.5 and 62.1 dyn/cm (Table 3). Since the surfactant is anionic, the solid-liquid interfacial interaction remained unaltered by the addition of surfactant except for the possibility of removing surface contamination, which would expose more silica, potentially increasing the solid-liquid contact area [*Wahlgren et al.*, 1993].

The experimental chamber consisted of two glass panels (50 cm wide × 60 cm high), separated by a 0.95-cm-thick acrylic spacer along the sides and bottom. The chamber was packed with air-dried sand using a prismatic funnel that fit the full width of the chamber. This funnel contained a series of coarse sieves which randomized particle motion as the sand fell into the chamber to generate a homogeneous packing. The chamber packing was conducted in one continuous pouring to prevent local gradations in particle size, which were observed to form when particle flow was interrupted during packing. The mass of sand and the packing height were recorded for each experiment and used to calculate the average porosity.

Fingers were generated by applying the liquids at a point at the sand surface with constant flow provided using a metering

Table 3. Measured Interfacial Tensions for Dilute SDS Surfactant Solutions

Molarity SDS	Number of Measurements	Air/Liquid Interfacial Energy σ(s.d.), dyn/cm
0.001	5	62.1 (1.4)
0.002	7	51.9 (1.7)
0.004	4	44.2 (0.5)
0.006	6	37.5 (0.3)

Table 4. Summary of NAPL Experiments

Experiment/Run	NAPL	Sand	Q_w, mL/min	Q_N, mL/min	d_w (s.d.), cm	d_N (s.d.), cm
1	S	30/40	3.94	0.68	1.69 (0.13)	2.38 (0.31)
2/1	S	40/50	1.54	0.57	5.24 (0.50)	4.70 (0.31)
2/2	...	40/50	1.54	...	7.26 (0.75)	...
3	S	12/20	5.45	1.39	1.69 (0.13)	1.42 (0.21)
4	S	20/30	4.20	1.19	2.88 (0.19)	2.12 (0.15)
5/1	S	12/20	4.97	1.34	0.84 (0.23)	1.44 (0.36)
5/2	S	12/20	4.97	1.34	1.12 (0.23)	1.21 (0.20)
6/1	S	20/30	4.40	1.09	1.52 (0.19)	1.59 (0.21)
6/2	S	20/30	4.40	1.09	1.42 (0.24)	1.61 (0.20)
8/1	S	30/40	3.21	0.65	2.88 (0.24)	2.36 (0.28)
8/1	S	30/40	3.21	0.65	2.80 (0.17)	2.67 (0.18)
10	S	40/50	1.18	0.25	4.37 (0.83)	4.01 (0.18)
11	S	20/30	4.04	0.97	1.60 (0.27)	1.61 (0.16)
12	S	40/50	0.80	0.20	5.81 (0.66)	3.25 (0.28)
13/1	...	12/20	3.58	...	0.89 (0.17)	...
13/2	D	12/20	3.58	0.57	0.81 (0.26)	0.48 (0.11)
14/1	D	20/30	2.90	0.25	2.57 (0.17)	1.69 (0.29)
14/2	D	20/30	2.90	...	2.40 (0.19)	...
15	D	30/40	0.97	0.20	2.90 (0.39)	2.43 (0.44)
16	D	40/50	...	0.20	...	3.73 (0.84)
17/1	D	12/20	2.84	0.45	1.04 (0.24)	0.96 (0.24)
17/2	D	12/20	2.84	0.45	0.92 (0.24)	0.93 (0.14)
18/1	D	20/30	4.27	0.25	1.85 (0.17)	1.52 (0.20)
18/2	D	20/30	4.27	0.25	1.74 (0.15)	1.71 (0.22)
19/1	D	30/40	2.50	0.30	3.22 (0.44)	2.14 (0.29)
19/2	D	30/40	2.50	...	3.19 (0.29)	...
20/1	D	40/50	...	0.22	...	2.82 (0.16)
20/1	D	40/50	...	0.22	...	3.55 (0.31)

D, Duoprime; S, Soltrol; Q_w, flux of water employed; Q_N, flux of NAPL employed; d_w and d_N, water and NAPL finger widths, respectively.

piston pump. Flow rates were established such that the flux in the fingers would be approximately an order of magnitude less than the saturated conductivity of the medium for that liquid in a finger of the dimensions predicted using (1). Twenty-four chamber packings were employed, with up to five fingers generated in each sand pack. In NAPL experiments at least one water finger and one NAPL finger were formed in each sand pack. A total of 59 usable fingers were generated (discarding experiments where adjacent fingers merged) (Table 4). Finger contours were traced onto acetate sheets attached to the front glass panel of the chamber for analysis. Finger width was characterized by measuring the width at 10 equally spaced intervals along the height of each finger, from which mean and standard deviation were calculated.

3. Results and Discussion

Water has been the liquid most widely investigated in Miller scaling to date. Considering the effect of media texture on the dimensions of fingers generated with pore water, we see that the unscaled media provided a range of finger diameters over a factor of 5.45 between sands, while media scaling reduced this variability to a factor of 1.72 (Tables 5 and 6). A simple measure of the degree to which a given scaling method explains observed variation is to consider the value of the coefficient of variation (CV) between experimental findings. In this case we note that the CV among water-generated fingers in the four media was 0.70 without media scaling, dropping to 0.24 when the effects of characteristic grain size were included. This reduction in variation between unscaled and scaled finger dimensions was equally dramatic for the NAPLs, with CVs dropping by no less than a factor of 3.6 (Table 6), supporting the widely used scaling procedures that have been found to explain variability in hydrodynamic processes between similar media.

Scaling based on liquid density (which differed only by 19% between the liquids), maintained or improved the consistency of the scaled dimensions in all but the 12/20 sand and thus appears to provide at least some of the expected benefits of scaling (Table 7). There were no systematic trends in finger

Table 5. Summary of Widths Obtained in NAPL and Water Fingered Flow Experiments

	12/20		20/30		30/40		40/50		
Liquid	Width, cm	n	Width, cm	n	Width, cm	n	Width, cm	n	CV
Water (s.d.)	1.04 (0.31)	7	1.99 (0.55)	8	2.78 (0.56)	6	5.67 (1.21)	4	0.70
Soltrol (s.d.)	1.36 (0.13)	3	1.73 (0.26)	4	2.47 (0.17)	3	3.99 (0.73)	3	0.49
Duoprime (s.d.)	0.79 (0.27)	3	1.64 (0.1)	3	2.29 (0.02)	2	3.37 (0.48)	1	0.54
CV	0.27		0.10		0.10		0.27		0.54

The number of repetitions of each measurement is listed as n.

Table 6. NAPL and Water Finger Width Results Scaled With Media Characteristic Length, Relative to 12/20

Liquid	12/20	20/30	30/40	40/50	CV
Water	1.04	1.29	1.33	1.81	0.24
Soltrol	1.36	1.12	1.19	1.28	0.08
Duoprime	0.79	1.07	1.10	1.08	0.15
CV	0.27	0.10	0.10	0.27	···

Table 8. NAPL and Water Finger Width Results Scaled With Gas-Liquid Interfacial Tension, Relative to Pore Water

Liquid	12/20	20/30	30/40	40/50	CV
Water	1.04	1.99	2.78	5.67	0.70
Soltrol	0.49	0.63	0.90	1.45	0.49
Duoprime	0.33	0.69	0.96	1.42	0.54
CV	0.60	0.70	0.69	0.86	···

dimension with liquid viscosity, which varied by more than a factor of 10 between water and Duoprime, as predicted by (1) (Table 6).

Quite different results were obtained when scaling was carried out based on the variation in gas-liquid interfacial tension. Considering first the comparison of "pure" liquids, Table 8 shows that inclusion of the gas-liquid interfacial tension exaggerated the discrepancies between experiments rather than explaining the variation in finger dimension. The CVs increased by a minimum of a factor of 2 compared to the unscaled data. Inclusion of both liquid properties found in (1) density and interfacial tension) improved upon the scaling based solely on interfacial tension, supporting the above observation that density effects appear to be correctly identified in (1) (Table 9).

To shed light on the shortcoming of scaling with respect to interfacial tension, we now consider the results obtained from altering the gas-liquid interfacial tension of the water through addition of the anionic surfactant SDS. Experimentally, changes in gas-liquid interfacial tension had little effect on the finger dimension (Table 10). For example, in 20/30 sand finger dimensions varied by only 15% while the interfacial tension varied by 66%, with the largest finger being found in the experiment with the lowest interfacial tension, the opposite of that predicted by (1). If we consider the observed variability in finger width through the eight combinations of conditions, the CV for the raw finger width data is 0.25. By scaling according to (1) for media characteristic length only, the CV reduces to 0.10, indicating that media scaling accounts for about 60% of the variability observed. On the other hand, scaling for interfacial tension actually increases the CV for the scaled finger dimensions, as observed previously for the NAPL fingers, indicating that the relationship between interfacial tension and finger dimension provided in (1) is not observed in these data.

The source of this discrepancy between (1) and the experimental data is deceptively simple: the gas-liquid interfacial tension scaling relationship provided in (1) depends upon the contact angle being constant between experiments [*Miller and Miller*, 1956], an assumption which appears to be violated in our experiments. The scaling relationship provided by (1) arises because of the competing forces of capillary pressure across the wetting front and gravitational potential. Increasing the energy dissipation due to gravity by increasing the fluid density decreases the finger width. Conversely, increasing the energy dissipated through wetting by increasing gas-liquid interfacial tension increases finger width.

Although not often appreciated, for cases of nonzero contact angle the energy of wetting is only a function of the solid-liquid and solid-gas interfacial energies, while the gas-liquid interfacial tension is irrelevant. This can be seen immediately by combining two of the most common results of capillary theory: the Laplace equation for pressure across curved interfaces, and Young's equation for equilibrium contact angle [e.g., *Bear*, 1972, pp. 442–445]. The Laplace equation for pressure across a curved capillary interface, P_c, is given by

$$P_c = \frac{2\sigma_{gl} \cos \gamma}{r} \tag{2}$$

where r is the effective radius of the capillary aperture, σ_{gl} is the gas-liquid interfacial tension, and γ is the liquid-solid-gas contact angle. Young's equation for contact angle may be stated as

$$\cos \gamma = \frac{\sigma_{sg} - \sigma_{sl}}{\sigma_{gl}} \tag{3}$$

where the subscript sg indicates the solid-gas interfacial tension, and sl indicates the solid-liquid interfacial tension. Substituting the expression for $\cos\gamma$ from (3) into (2), we see that the pressure drop across the capillary interface is given by

$$P_c = \frac{2(\sigma_{sg} - \sigma_{sl})}{r} \tag{4}$$

which depends only upon the interfacial tension between the gas-solid and solid-liquid pairs. SDS, being an anionic surfactant, does not affect the gas-solid interfacial tension [*Wahlgren et al.*, 1993]. Thus from (4) the capillary pressure across the gas-liquid interface is expected to be unaffected. Since it is precisely this capillary pressure which influences the finger width, as long as the contact angle is nonzero, the gas-liquid interfacial tension is unrelated to finger width. Remarkably, this fact is overlooked in most treatments of (2) in standard texts, where σ and γ are considered to be essentially independent parameters [e.g., *Jury et al.*, 1991].

Table 7. NAPL and Water Finger Width Results Scaled With Liquid Density, Relative to Pore Water

Liquid	12/20	20/30	30/40	40/50	CV
Water	1.04	1.99	2.78	5.67	0.70
Soltrol	1.68	2.14	3.05	4.93	0.49
Duoprime	0.92	1.91	2.66	3.92	0.54
CV	0.34	0.06	0.07	0.18	···

Table 9. NAPL and Water Finger Width Results Scaled With Media Characteristic Length, Liquid Density, and Gas-Liquid Interfacial Tension, Relative to Pore Water

Liquid	12/20	20/30	30/40	40/50	CV
Water	1.04	1.29	1.33	1.81	0.24
Soltrol	0.61	0.50	0.53	0.57	0.08
Duoprime	0.39	0.52	0.54	0.53	0.15
CV	0.49	0.58	0.58	0.75	···

In a heterogeneous porous medium there is no single contact angle but rather a statistical distribution associated with the varied surfaces found in the medium. An ascribed contact angle for a medium must be recognized as an effective parameter. We know that as the gas-liquid interfacial tension decreases, the contact angle also decreases. Had the effective contact angle become zero beyond some critical interfacial tension value, it would have been expected that the Miller-scaling result would hold for all lower interfacial tensions. We see no evidence of this behavior here and therefore must conclude that the effective contact angle for the media was nonzero at least to the lowest gas-liquid interfacial tension tested. If we were to suppose that the contact angle was zero for solutions with surface tension lower than the 0.006 M SDS solution (i.e., that $\sigma_{sg} - \sigma_{sl} \geq \sigma_{gl}$), the contact angle for pore water may be computed using (3) to be greater than or equal to 58°, significantly departing from the typically assumed value of zero.

Evaluation of the effective contact angle of the fluids on the sands was undertaken using the set-up shown in Figure 1. Twelve of the 26 grains tested had nonzero contact angle with pure water. It was also observed that the time required to achieve full wetting of the 14 grains which did have zero contact angle was typically between 5 and 15 s. This suggests that the effective contact angle is a function of the rate of infiltration, which could explain some of the enlarging finger dimensions under low infiltration behavior found by *Hendrickx and Yao* [1996]. Of the 12 grains that had nonzero contact angle with pure water, six continued to have nonzero contact angle with 0.001 M SDS, and five had non zero contact angle with 0.006 M SDS. This was determined by repeating the experiment with the same sand grains using 0.001 M and 0.006 M solutions successively, allowing the grain to dry between experiments. Since the surfactant in the 0.001 M solution remained on the sand grains, the effective solution strength during the 0.006 M trials could have been closer to 0.007 M, which does not affect the qualitative conclusions of these tests. For the grains that did not wet, the advancement of the liquid surface appeared to be obstructed by physical defects on the sand surface. These results are consistent with the fingered flow experiments, which find that contact angle is nonzero for pure water and that a decreasing gas-liquid interfacial tension does reduce the effective contact angle.

4. Conclusions

We have shown that Miller scaling for media texture is an effective means of explaining the hydrodynamic behavior of liquids in porous media, and the effects of liquid density and viscosity are well predicted. In accounting for the effects of interfacial tension, on the other hand, Miller scaling based on the typical assumption of zero contact angle did not provide accurate prediction of observed behavior. It appears that the effective contact angle of the liquid-solid pair was variable in the infiltration process, violating a key assumption of Miller-scaling. This was unexpected for a very clean, low-organic-matter silica sand but was confirmed in wetting tests on single sand grains. Further experiments will be required to fully understand these observations, but these results would suggest that the use of interfacial tension scaling is not advisable in many cases and that the widely employed assumption of zero contact angle is not justified. The observation of slow wetting of individual sand grains suggests that the effective contact angle is typically far from zero and related to the rate of advance of the wetting process. Previous research by *Glass et al.* [1989] found that finger dimensions stabilized at low infiltration rates, which is at odds with this conclusion. The recent result of *Hendrickx and Yao* [1996], however, suggests that finger dimensions increase when infiltration is extremely slow, which may be explained by the expected reduction in contact angle as dynamic effects are minimized.

Table 10. SDS Fingered Width Results, Scaled to 12/20 Sand and Pore Water

SDS	Sand	Q, mL/min	n[a]	d,[b] cm	$d\lambda$,[c] cm	d/σ,[d] cm	$\lambda d/\sigma$,[e] cm
0.001	20/30	4.1	2	1.09	0.71	1.25	0.81
0.002	20/30	4.1	2	1.08	0.71	1.48	0.96
0.004	20/30	4.5	2	1.15	0.75	1.85	1.21
0.006	20/30	4.5	2	1.26	0.82	2.40	1.56
0.001	30/40	3.6	1	1.92	0.92	2.20	1.06
0.002	30/40	3.6	1	1.81	0.89	2.49	1.19
0.004	30/40	3.6	1	1.72	0.83	2.77	1.33
0.006	30/40	3.2/3.6[f]	2	1.82	0.87	3.46	1.66
CV	...	...		0.25	0.10	0.32	0.23

[a]Number of replicates.
[b]Average measured finger diameter.
[c]Average measured finger diameter scaled to the 12/20 characteristics length.
[d]Average measured finger diameter scaled to the surface tension of pore water.
[e]Average measured finger diameter scaled to the surface tension of pore water and the 12/20 characteristic length.
[f]The two fingers had differing fluxes, as indicated.

Acknowledgments. We thank Arron Burkhart and Darren Lerner, who provided invaluable assistance in completing the experiments described; the U.S. Department of Energy Subsurface Science Program for their support of this work under contract DE-FG06-92-ER61523; and the constructive reviews provided by J. M. H. Hendrickx and R. A. Birchwood.

References

American Society for Testing and Materials, Standard test method for kinematic viscosity of transparent and opaque liquids (the calculation of dynamic viscosity), *Designation D 445–94, Am. Natl. Stand., Annu. Bk. ASTM Stand., 05.01*, pp. 160–167, Washington, D. C., 1995.

Bear, J., *Dynamics of Fluids in Porous Media*, Dover, Mineola, N. Y., 1972.

Downey, J., and C. C. Addison, The properties of detergent solutions, II, The surface and interfacial tensions of aqueous solutions of alkyl sodium sulphates, *Trans. Faraday Soc., 33*, 1243–1260, 1937.

Du Noüy, P. L., A new apparatus for measuring surface tension, *J. Gen. Physiol., 1*, 521–524, 1919.

Glass, R. J., and M. J. Nicholl, Physics of gravity fingering of immiscible fluids within porous media: An overview of current understanding and selected complicating factors, *Geoderma, 70*, 133–163, 1996.

Glass, R. J., T. S. Steenhuis, and J.-Y. Parlange, Wetting front instability, 2, Experimental determination of relationships between system parameters and two-dimensional unstable flow field behavior in initially dry porous media, *Water Resour. Res., 25*, 1195–1207, 1989.

Hendrickx, J. M. H., and T.-M. Yao, Prediction of wetting front stability in dry field soils using soil and precipitation data, *Geoderma, 70*, 265–280, 1996.

Hillel, D., and D. E. Elrick (Eds.), *Scaling in Soil Physics: Principles and Applications, Spec. Publ. 25*, Soil Sci. Soc. of Am., Madison, Wis., 1990.

Jury, W. A., W. R. Gardner, and W. H. Gardner, *Soil Physics*, 5th ed., John Wiley, New York, 1991.

Miller, E. E., and R. D. Miller, Physical theory for capillary flow phenomena, *J. Appl. Phys.*, *27*, 324–332, 1956.

Parlange, J.-Y., and D. E. Hill, Theoretical analysis of wetting front instability in soils, *Soil Sci.*, *122*, 236–239, 1976.

Schroth, M. H., S. J. Ahearn, J. S. Selker, and J. D. Istok, Characterization of Miller-similar sands for laboratory hydrologic studies, *Soil Sci. Soc. Am. J.*, *60*, 1331–1339, 1996.

Selker, J. S., T. S. Steenhuis, and J.-Y. Parlange, Wetting front instability in homogeneous sandy soils under continuous infiltration, *Soil Sci. Soc. Am. J.*, *56*, 1346–1350, 1992.

Wahlgren, M. C., T. Arnebrant, A. Askendal, and S. Welin-Klinstöm, The elutability of fibrinogen by sodium dodecyl sulphate and alkyltrimethylammonium bromides, *Colloids Surf. A*, *70*, 151–158, 1993.

M. H. Schroth, Department of Civil, Construction and Environmental Engineering, Oregon State University, Apperson Hall, Corvallis, OR 97331.

J. S. Selker, Department of Bioresource Engineering, Oregon State University, Gilmore Hall, Rm. 240, Corvallis, OR 97331-3906. (e-mail: selkerj@engr.orst.edu)

(Received February 25, 1997; revised February 10, 1998; accepted February 18, 1998.)